Conformational Dynamics of the Cytochrome P450 BM3/ N -Palmitoylglycine Complex: The Proposed "Proximal−Distal" Transition Probed by Temperature-Jump Spectroscopy

ARTICLE *in* THE JOURNAL OF PHYSICAL CHEMISTRY B · AUGUST 2007

Impact Factor: 3.3 · DOI: 10.1021/jp073036n · Source: PubMed

5 AUTHORS, INCLUDING:

Sam Hay
The University of Manchester
68 PUBLICATIONS **1,108** CITATIONS
SEE PROFILE

Andrew W Munro
The University of Manchester
206 PUBLICATIONS **5,368** CITATIONS
SEE PROFILE

Nigel S Scrutton
The University of Manchester
346 PUBLICATIONS **7,849** CITATIONS
SEE PROFILE

Conformational Dynamics of the Cytochrome P450 BM3/*N*-Palmitoylglycine Complex: The Proposed "Proximal−Distal" Transition Probed by Temperature-Jump Spectroscopy

Sibylle Brenner, Sam Hay, Hazel M. Girvan, Andrew W. Munro, and Nigel S. Scrutton*

Manchester Interdisciplinary Biocentre and Faculty of Life Sciences, University of Manchester, 131 Princess Street, Manchester M1 7DN, United Kingdom

Received: April 19, 2007

The ferric spin state equilibrium of the heme iron was analyzed in wild-type cytochrome P450 BM3 and its F87G mutant by using temperature (T)-jump relaxation spectroscopy in combination with static equilibrium experiments. No relaxation process was measurable in the substrate-free enzyme indicating a relaxation process with a rate constant $\gg 10\,000\ s^{-1}$. In contrast, a slow spin state transition process was observed in the *N*-palmitoylglycine (NPG)-bound enzyme species. This transition occurred with an observed rate constant (298 K) of $\sim$800 s^{-1} in the wild-type, and $\sim$2500 s^{-1} in the F87G mutant, suggesting a significant contribution of the phenylalanine side chain to a reaction step rate limiting the actual spin state transition. These findings are discussed in terms of an equilibrium between different binding modes of the substrate, including a position 7.5 Å away from the heme iron ("distal") and the catalytically relevant "proximal" binding site, and are in accordance with results from X-ray crystallography, NMR studies, and molecular dynamics simulations.

Introduction

Cytochromes P450 (P450s) are a superfamily of *b*-type heme-containing enzymes. They are usually mono-oxygenases, catalyzing a huge variety of oxidative transformations such as the detoxification of xenobiotics by the mammalian hepatic isoforms, and steps in the biosynthesis of signaling molecules such as prostaglandins.[1] A complex multistep catalytic cycle is involved, resulting in the activation of molecular oxygen bound to the P450 heme iron and insertion of an atom of oxygen into a substrate.[2,3] In the resting state, the P450 absorbance spectrum of the ferric heme is dominated by a Soret (γ) band around 418 nm, which, upon substrate binding, is blue-shifted to $\sim$390 nm.[4−6] This so-called type I spectral change[7,8] was assigned to the transition of the ferric heme iron from the resting low-spin (LS, $S = {}^1/_2$) state with a water molecule as the sixth ligand[9,10] to the 5-coordinated[11] high-spin (HS, $S = {}^5/_2$) species.[12] Upon the LS-to-HS transition, the reduction potential of the heme iron shows a positive shift of around 130−140 mV,[11,13−16] enabling electron uptake from the redox partner and allowing the catalytic cycle to proceed. Following the reduction of the heme iron to the ferrous state, molecular oxygen binds and the ferrous-dioxy (isoelectric with the ferric-superoxy) intermediate is formed. Introduction of a second electron from the redox partner and two protons leads to the splitting of the oxygen and the release of a water molecule. The resulting high valent oxo-iron species (commonly termed compound I) rapidly collapses, forming oxygenated product and (once water rebinds to the ferric iron) returning the enzyme to the resting form. Thus, the coupling of substrate binding (NPG in this study) and redox potential provides an important thermodynamic[11,13−17] as well as kinetic[17−20] switch preventing the wastage of reducing equivalents in uncoupling reactions to form superoxide, hydrogen peroxide, or water in the absence of substrate.[21]

Spectral changes associated with spin state transitions are not only observed upon substrate binding. A temperature-sensitive spin state equilibrium is also detectable in the absence of substrate and at substrate saturation, with low temperatures generally favoring the LS state.[13,14,22−24] This temperature-dependent spectral equilibrium provides an ideal enzymatic system to be investigated by temperature-jump (T-jump) relaxation spectroscopy in combination with static equilibrium experiments, as indicated by several T-jump studies on P450s during the last few decades (see, e.g., refs 14 and 24−30).

The P450 family member most extensively examined by T-jump spectroscopy is CYP101A1 (P450 cam), a camphor hydroxylase from *Pseudomonas putida*.[14,24,25,29] One major question tackled in these T-jump experiments was whether substrate binding and the LS-HS transition are simultaneous events. The dependence of the relaxation rates on the substrate concentration is expected to yield a linear relationship in the case of a simple bimolecular binding equilibrium[31,32] ($E^{LS} + S \rightarrow E^{HS}S$), while saturation behavior is predicted in the three-state model[33] involving a substrate-bound spin state equilibrium ($E^{LS} + S \rightarrow E^{LS}S \rightarrow E^{HS}S$). The latter model evolved from the four-state model,[14] in which the substrate can be bound by either LS or HS enzyme. While the simple two-state equilibrium was proposed for cytochrome CYP2B4 (formerly known as P450 LM2),[26,27,34] conflicting findings were reported for P450 cam, resulting either in a linear behavior indicative of the two-state model[29] or in saturation behavior.[25]

With advances in P450 biochemistry driven by techniques such as X-ray crystallography, solid-state NMR, and molecular dynamics simulations, spin state transitions can now be interpreted from the wealth of structural information that was unavailable during the early days of P450 research. For instance, interesting structural differences have been observed between various P450s cocrystallized with their respective substrates. Some enzyme−substrate complexes, such as those for P450 cam[35−37] and for the mammalian P450s CYP2C5[38,39] and CYP2C9,[40] showed the substrate bound at a position close to

* Address correspondence to this author. E-mail: nigel.scrutton@manchester.ac.uk.

10.1021/jp073036n CCC: $37.00
Published on Web 06/16/2007

the heme iron (≤4 Å for P450 cam[35−37]), which is likely to be the catalytically relevant binding conformation. In contrast, other substrate-bound P450s featured substrate-binding conformations too distant (>6 Å) from the heme for oxidative catalysis to occur. In the structure of progesterone-bound CYP3A4, for instance, the steroid was located in what is considered to be a preliminary binding mode, requiring conformational readjustments (perhaps effected by binding of redox partners cytochrome P450 reductase or cytochrome b_5) to facilitate movement of the substrate to the active site.[41]

For the flavocytochrome CYP102A1 (P450 BM3 or BM3) from *Bacillus megaterium*, a fatty-acid hydroxylase in which the P450 is fused to its cytochrome P450 reductase redox partner, a number of different structures are available for the heme (P450) domain, in both the presence and absence of substrate. An early structure of a palmitoleate-bound heme domain showed the poorly resolved substrate 7.5−7.9 Å from the heme iron,[42] which was in accordance with NMR relaxation experiments on the laurate-bound heme domain that yielded a distance of ∼7.6 Å.[43] More recently, a high-resolution structure of the BM3 heme domain was obtained with the substrate *N*-palmitoylglycine (NPG) also bound at a position 7.5 Å "distal"[44] from the heme iron,[45] i.e., in a noncatalytic position analogous to that seen in the progesterone-bound CYP3A4 structure.[41] In the NPG binding mode observed for BM3, the side chain of amino acid Phe87 was shown to separate the NPG molecule from the heme. The phenyl ring of this residue is considered to interact with the ω-methyl group of the substrate and to prevent BM3 oxygenating fatty acids at this position.[42] Haines et al. suggested that a water molecule switched between the sixth coordination position on the heme iron, where it favors the LS state, and a binding position in the I-helix, where it is stabilized by hydrogen bonding to the conserved residues Thr268 and Ala264.[45] The authors concluded that the spin state equilibrium at room temperature might result from partitioning of this water molecule between the two binding sites.[45] However, for catalysis to occur, the ω end of the fatty acid has to bind much closer (more "proximal"[44]) to the heme than is observed in the NPG-bound structure,[43,44,46] i.e., with relevant C−H bonds orientated close to the heme iron, as is seen for the binding of camphor to P450 cam.[11] In an attempt to resolve this apparent inconsistency, the NPG-bound crystal structure was used as a starting point for solid-state NMR and molecular dynamics studies, which suggested that an entropically driven reorientation of the substrate (i.e., a distal-to-proximal transition) involving a conformational change of Phe87 might shift the spin state equilibrium further toward the HS species.[44,47−49] These studies indicated that the temperature-sensitive spin state equilibrium in BM3 might not only emerge from the water molecule binding alternately to the heme iron and to the I-helix, but also from a conformational conversion between different substrate binding modes.

To investigate whether the postulated repositioning of the substrate is reflected in the kinetic behavior of spin state conversions, we analyzed spin state transitions in the substrate-free as well as the NPG-bound BM3 heme domain (wtBM3)[50] using T-jump relaxation kinetics in combination with equilibrium absorbance spectroscopy. The isolated heme domain has been shown to exhibit highly similar substrate- and ligand-binding properties by comparison with the respective domain in the full-length flavocytochrome,[50] and thus the BM3 heme domain presents a reliable and easily interpretable model system. To verify the postulated influence of Phe87 on the spin state equilibrium in the NPG-bound enzyme,[44,47−49] the kinetic and static effects of temperature on heme iron spin state in the F87G mutant (BM3-F87G)[51] were also examined, and results were compared with data obtained for the wild-type enzyme.

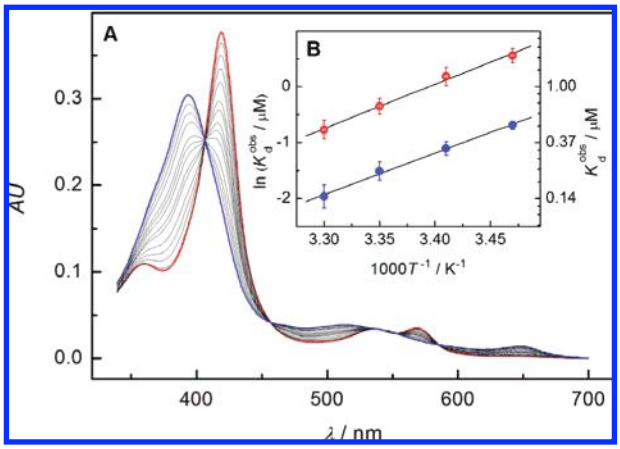

Figure 1. (A) Spectral changes associated with the binding of NPG to wtBM3 at 298 K: (red) substrate-free LS enzyme (4 μM), (blue) after the addition of 9.24 μM NPG, and (black) selected intermediate spectra. K_d^{obs} values were obtained by plotting the absorbance at 419 nm and analyzed by using a quadratic binding equation (eq 1). A representative graph is shown in the Supporting Information (Figure S1). (B) van't Hoff plots for the binding of NPG to wtBM3 (blue) and BM3-F87G (red). The data were analyzed by using eq 2 and the resulting ΔH and ΔS values are given in the text.

Results

Binding of NPG to wtBM3 and BM3-F87G. To establish whether it was possible to measure the binding/dissociation of NPG by T-jump relaxation spectroscopy, binding titrations of NPG to the wtBM3 and its F87G mutant were performed at various temperatures ranging from 288 to 303 K. The spectral shift of the Soret maximum from 419 to 395 nm associated with substrate binding was used to determine spectroscopic (observed) dissociation constants ($K_d^{obs} = [E^{LS}][S]/[E^{HS}S]$) (Figure 1A) and the decrease in absorbance at 419 nm was analyzed by using a quadratic binding equation (eq 1 in the Experimental Section, Supporting Information, Figure S1). For wtBM3, the observed dissociation constant at 298 K was 220 ± 40 nM, which is in good agreement with the published value of 262 nM.[45] BM3-F87G exhibited higher observed dissociation constants throughout the experimental temperature range with a K_d^{obs} value of 700 ± 100 nM at 298 K, which is ∼3-fold weaker than that for the wild-type enzyme. The temperature dependence of the dissociation constants was analyzed in a van't Hoff plot (Figure 1B, eq 2 in the Experimental Section) allowing the calculation of the reaction enthalpies (ΔH) and entropies (ΔS). Binding of NPG to both the wild-type and F87G enzymes was favored at elevated temperatures yielding positive reaction enthalpies of 61 ± 2 and 66 ± 3 kJ mol^{-1}, respectively. Positive reaction entropies (ΔS = 333 ± 5 and 338 ± 11 J mol^{-1} K^{-1} for wtBM3 and BM3-F87G, respectively) resulted in a significant enthalpy−entropy compensation with reaction energies of ΔG(298K) = −38 ± 3 and −35 ± 7 kJ mol^{-1}, respectively. Evaluation of the dissociation constants demonstrated that the extremely tight binding of NPG to BM3 did not allow for examination of the actual binding event in a T-jump experiment due to the high enzyme concentrations (∼40 μM) needed for a measurable absorbance change in the 3 mm path length cell of the T-jump instrument. Consequently, even substoichiometric NPG concentrations were expected to be fully bound to the enzyme under accessible experimental conditions.

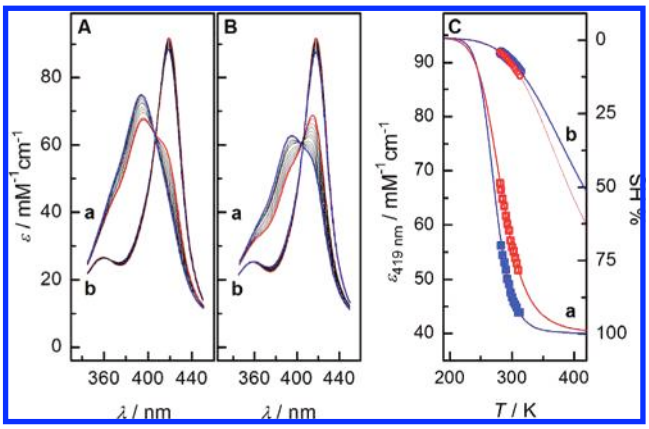

Figure 2. Temperature dependence of the spin state equilibria of the wtBM3 (A) and BM3-F87G (B) in the presence (a) and absence (b) of saturating NPG. The red and blue spectra were recorded at 283 and 313 K, respectively, with the black spectra taken at intermediate temperatures. (C) Temperature dependence of the extinction coefficients at 419 nm. Blue closed circles: substrate-free wtBM3; red open circles: substrate-free BM3-F87G; blue closed squares: NPG-saturated wtBM3; and red open squares: NPG-saturated BM3-F87G. The solid lines are fits to eq 3 with ϵ_{LS} and ϵ_{HS} fixed to 94.5 and 40 mM^{-1} cm^{-1}, respectively, at 419 nm—see text for details. The right ordinate shows the percentage of HS enzyme corresponding to the respective extinction coefficient.

Static Temperature Dependence of the Ferric Spin State Equilibria in the Presence and Absence of NPG. Static spin state equilibrium constants were determined for the substrate-free wtBM3 and BM3-F87G, as well as for the NPG-saturated enzyme species, by measuring the temperature dependence of absorption changes in the Soret region in a temperature range from 283 to 313 K (Figure 2). Clear isosbestic points were observed in all data sets at 407 nm for the substrate-free P450, and at 405 nm for the NPG-bound P450. The spectra were analyzed by plotting the observed extinction coefficient (at 419 nm) versus the absolute temperature and by fitting the data to eq 3 in the Experimental Section (Figure 2C). Since the final levels for the extinction coefficients of pure LS and pure HS enzyme were ill-defined for the NPG-bound and the substrate-free case, respectively, the extinction coefficient of pure LS enzyme was fixed to $\epsilon_{419} = 94.5$ mM^{-1} cm^{-1} (resulting from the regression of substrate-free wtBM3, which is in good agreement with published values[52]) and to $\epsilon_{419} = 40$ mM^{-1} cm^{-1} for pure HS enzyme (resulting from the regression of NPG-bound wtBM3). The obtained reaction parameters ΔH and ΔS could then be used to estimate the spin state equilibrium constants ($K_{eq} = [E^{HS}]/[E^{LS}]$, $K_{eq}^{sub} = [E^{HS}S]/[E^{LS}S]$) for any temperature, which is a prerequisite to extract microscopic rate constants from observed rate constants measured in T-jump experiments. The degree of HS enzyme was found to be lower than 10% for the substrate-free wtBM3 and lower than 12% for BM3-F87G throughout the experimental temperature range, resulting in an inversion temperature, T_{inv} (when $K_{eq} = 1$), of 367 K for the mutant compared to 381 K for the wild-type. In contrast, the HS content of the NPG-bound wtBM3 spanned a range from 65% to >90% and from ~50% to ~80% for BM3-F87G. Hence, the spin state equilibrium of the NPG-bound F87G mutant was slightly shifted toward the LS state compared with wtBM3 yielding an inversion temperature of 281 K, which is 10 K higher than that for the wild-type. This suggests that the energetic bias toward the HS state is less pronounced for the NPG-bound mutant than for the NPG-bound wild-type enzyme. These observations were reflected in the reaction free energies, which were positive for the substrate-free enzyme species ($\Delta G(298K) = 6.1 \pm 0.4$ and 5.9 ± 0.3 kJ mol^{-1} for wtBM3 and BM3-F87G, respectively) and negative for the NPG-bound spin state transitions ($\Delta G(298K) = -4 \pm 3$ and -2 ± 1 kJ mol^{-1} for wtBM3 and BM3-F87G, respectively). Although the conversions of the LS to the HS enzyme species were exergonic in the presence of NPG, the reaction enthalpies of 45 ± 1 and 33 ± 0.5 kJ mol^{-1} for the NPG-bound wild-type and F87G enzymes, respectively, were found to be even more unfavorable than the values of 21.9 ± 0.2 and 25 ± 0.7 kJ mol^{-1}, respectively, obtained in the absence of substrate. Thus, as for the case of the binding titrations, considerable enthalpy−entropy compensation was observed for both the substrate-free and the NPG-bound equilibrium, while the favorable entropy term prevailed for the substrate-bound transitions, shifting the equilibrium toward the HS state.

T-Jump Experiments. The dynamic aspects of the temperature-dependent spin state equilibria were examined for substrate-free and NPG-bound wtBM3 and for NPG-bound BM3-F87G, using T-jump relaxation absorbance spectroscopy. Kinetic traces were collected applying a T-jump of approximately 10 K[53] and absorbance changes were monitored at single wavelengths.

T-Jump of Substrate-Free wtBM3. Analyzing the substrate-free spin state equilibrium in wtBM3 with a time constant (t_c) of 0.1 ms (see below) did not yield any observable relaxation amplitude after averaging more than 40 traces (Figure 3A, black trace). When a time constant of 1 ms was used, a relaxation process was measurable due to the improved signal-to-noise ratio, but the apparent rate constants were limited by the detector speed, i.e., $k_{obs} \approx 1000$ s^{-1} ($1/t_c$, data not shown). These findings indicated that the actual relaxation process was much faster than 10 000 s^{-1} ($1/t_c$) and was undetectable due to the diminished signal-to-noise ratio associated with lower time constants. To obtain an action spectrum of the substrate-free spin state equilibrium (Figure 3B, black data), a time constant of 10 ms yielding apparent rate constants of ~100 s^{-1} was used (Supporting Information, Figure S2) and traces were collected at various wavelengths around the Soret band. The observed relaxation amplitudes corresponded to approximately 90% of the absorbance change expected from the static experiments. The significant correlation with the normalized static difference spectrum confirmed that the ferric spin state transition was observed in the T-jump experiments. Consistently, maximum absorbance changes were detected at 422 and 389 nm and an isosbestic point was observed at 407 nm. However, since no true rate constants could be measured, further analysis of the substrate-free spin state equilibrium in BM3 was not possible with use of a capacitor T-jump instrument.

T-Jump of NPG-Bound wtBM3. In contrast to the substrate-free T-jump experiments, the relaxation process of NPG-saturated wtBM3 (40 μM wtBM3, 80 μM NPG) exhibited a slow phase, which was observable after averaging only ~15 traces, and could be analyzed by single-exponential regression (Figure 3A, blue trace). For a T-jump of 10 K and a final temperature of 298 K, the observed rate constant was found to be 880 ± 60 s^{-1}. Since the traces were collected with a t_c of 0.1 ms, the process was not rate-limited by data acquisition ($1/t_c = 10\,000$ s^{-1}). The action spectrum could be overlaid with the normalized NPG-bound static difference spectrum and was blue-shifted by about 2 nm compared with the substrate-free case, yielding maximum absorbance changes at 420 and 387 nm, and an isosbestic point at 405 nm. Contrary to the substrate-free relaxation process, the magnitude of the observed relaxation amplitudes was only ~10% of the absorbance change detected in the static difference spectrum. Therefore, a significant

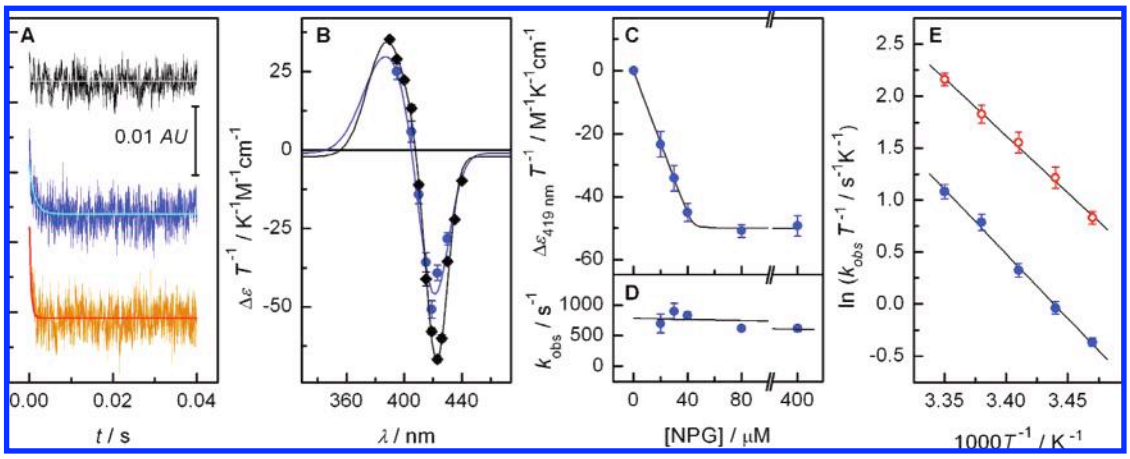

Figure 3. T-jump data. (A). T-jump traces for substrate-free (black) and NPG-bound (blue) wtBM3, and for the NPG-bound BM3-F87G (orange). All traces were collected with a start temperature of 288 K, a 10 K temperature jump, and a time constant of 0.1 ms with 15−40 traces averaged. The solid lines are fits to a single exponential, or to a straight line in the case of the substrate-free trace. (B) Action spectra for substrate-free (black) and NPG-bound (blue) wild-type BM3. Relaxation amplitudes for the NPG-bound enzyme were collected as described in panel A. The substrate-free action spectrum was obtained by using a time constant of 10 ms and analyzed single-exponentially with the observed rate constants being limited by the detector speed. The solid lines are fits of the corresponding equilibrium difference spectra, and the difference spectrum of the NPG-bound species is blue-shifted by ~2 nm compared with the substrate-free spectrum. (C and D) The effect of NPG concentration on the relaxation amplitudes (C) and observed rate constants (D) in wtBM3 (blue). Traces were collected and analyzed as described in panel A. The solid line in panel C results from a fit to eq 1 with a stoichiometry of ~1:1. The data in panel D were analyzed by using linear regression (solid line) with a slope of $-0.4 \pm 0.4\ \mu M^{-1}\ s^{-1}$. (E) Eyring plot of the observed rate constants for the NPG-bound wtBM3 (blue) and NPG-bound BM3-F87G (orange). Data were collected as in panel A, utilizing different starting temperatures, and are plotted versus the final temperature. Extracted $\Delta H^{\ddagger}$ and $\Delta S^{\ddagger}$ values are given in the text.

amplitude loss appears to occur within the instrument dead time (see Discussion). The degradation in signal-to-noise upon further decreasing the t_c prevented more detailed analysis of this amplitude loss.

The slow phase observed in NPG-bound wtBM3 was further examined by measuring the dependence of the relaxation amplitudes and k_{obs} on the NPG concentration, using a t_c of 0.1 ms (Figure 3C,D). As had been demonstrated by the static binding titrations, the extremely low observed dissociation constants of NPG and the high enzyme concentrations used for the T-jump experiments were expected to result in the binding of virtually all NPG molecules, as long as (sub)stoichiometric substrate concentrations were applied. Consistently, the observed rate constants were concentration independent and resulted in a linear dependence with a slope of $-0.4 \pm 0.4\ \mu M^{-1}\ s^{-1}$ (Figure 3D). Moreover, the relaxation amplitudes showed a strict correlation with the concentration of NPG-bound wtBM3 (Figure 3C): Only those enzyme molecules bound to NPG resulted in an observable relaxation amplitude, while the process of the substrate-free enzyme species had been shown to be undetectable with use of a t_c of 0.1 ms (see above). Hence, the concentration dependence did not reflect any kind of saturation behavior. As a consequence, the different spin state models suggested for P450 cam[25,29] could not be verified for BM3 with use of our approach. These results also emphasized the conclusion that the slow relaxation process only occurs in the NPG-bound enzyme species.

T-Jump of NPG-Bound BM3-F87G. The relaxation process in NPG-bound wtBM3 might be explained by a rate-limiting conformational change gating the actual spin state transition. As Phe87 was reported to undergo a significant conformational change accompanied by a repositioning of the NPG molecule[44,47−49] the kinetic behavior of the NPG-bound F87G mutant was analyzed by using the same conditions as for the wild-type enzyme. A 10 K T-jump with a final temperature of 298 K gave a single-exponential relaxation rate of $2600 \pm 150\ s^{-1}$ (Figure 3A, orange trace), which is significantly faster than the rate constant of $880 \pm 60\ s^{-1}$ observed for the wild-type enzyme.

To gain some more insight into the differential behavior of NPG-bound wtBM3 and BM3-F87G, the temperature dependence of the apparent rate constants was examined over a temperature range from 288 to 298 K (final temperatures). The obtained rate constants were analyzed in an Eyring plot (Figure 3E) yielding a linear behavior in both cases. The activation enthalpy $\Delta H^{\ddagger}$ was slightly more unfavorable for the wild-type than for the mutant enzyme ($\Delta H^{\ddagger} = 105 \pm 5$ and 94 ± 6 kJ mol^{-1}, respectively), which was found to be partly compensated for by the more favorable entropy term: $\Delta S^{\ddagger} = 162 \pm 8$ and 136 ± 8 J $mol^{-1}\ K^{-1}$ for wtBM3 and BM3-F87G, respectively. The positive activation entropies suggest that the transition state is less ordered than the ground state.

If the static spin state change at saturating NPG concentrations reflects the same process observed in the T-jump, the spin state equilibrium constants K_{eq}^{sub} can be used in combination with the observed rate constants to calculate microscopic rate constants for the forward (k_f; $E^{LS}S \rightarrow E^{HS}S$) and the reverse reaction (k_r) (eq 4 in the Experimental Section). By using this assumption, linear Eyring plots were obtained for k_f and k_r (data shown in the Supporting Information, Figure S3) and the higher rate for the LS to HS transition (k_f) was found to be entirely of entropic origin. However, the significant difference in the amplitudes of static and dynamic spin state transitions clearly indicated that the observed slow relaxation might not reflect the complete process. In that case, the spin state equilibrium constants may not be employed to analyze the observed rate constants.

Discussion

The molecule NPG used in this work has been reported to provide an excellent model substrate for P450 BM3, since it binds more tightly than the majority of fatty acids and also exhibits a much greater water solubility, thus reducing experimental flaws.[45] Our spectral titrations showed that binding is

favored at elevated temperatures and that the observed dissociation constant changes from 500 ± 40 nM at 288 K to 220 ± 40 nM at 298 K. The latter value is in good agreement with the published value of 262 nM.[45] Tighter binding upon a rise in temperature has also been observed for benzphetamine binding to CYP2B4.[26] The binding of NPG to BM3 was found to be entropically favorable, leading to substantial enthalpy−entropy compensation. The highly favorable reaction entropy upon binding may be due to the unfavorable reorganization of water molecules around fatty acids in aqueous solution, which has also been detected for other fatty acid-binding proteins.[54−56] Moreover, several water molecules were reported to be released from the substrate access channel upon the transition from LS to HS BM3, and these may also contribute to the positive entropy term.[45]

The spin state equilibrium constants determined for substrate-free as well as for the NPG-bound BM3 were also shown to be associated with a positive reaction enthalpy while being highly entropically favorable. In the case of the NPG-bound enzyme species, the energetic bias toward the HS state is entirely of entropic origin. Positive reaction enthalpies and entropies have been reported for spin state transitions in substrate-bound P450 cam, and the favorable entropy term associated with the transition from the LS to HS state has been attributed to the release of ordered water molecules from the active site in P450 cam.[25]

Using capacitor T-jump experiments, we were not able to determine true rate constants for the relaxation process in substrate-free wtBM3, indicating that spin state transitions are likely to occur much faster than 10 000 s^{-1}. Employing a time constant of 10 ms resulted in apparent rate constants limited by the detector speed; an action spectrum was obtained resembling the static difference spectrum and the signal amplitudes corresponded approximately to the statically determined spectral changes. Spin state transition rates of $k_{obs} \approx 5.5 \times 10^6$ s^{-1} have been reported for the substrate-free CYP2B4 by using a laser T-jump instrument,[30] while substrate-free cytochrome P450 cam yielded observed rate constants as low as 59 s^{-1}.[24] These observations suggest that the rates of spin state conversions might vary substantially between different members of the P450 enzyme superfamily.

Contrary to the data for substrate-free BM3, relaxation experiments with the NPG-saturated P450 could be performed by using a time constant of 0.1 ms and yielded observed rate constants between ~200 (288 K) and ~900 s^{-1} (298 K) for the NPG-bound wild-type enzyme. Due to the low K_d^{obs} values determined for NPG and the high enzyme concentrations of 40 μM used for the T-jump experiments, (sub)stoichiometric substrate concentrations were demonstrated to be bound to BM3 over the whole experimental temperature range. Therefore, the possibility that the detected temperature-dependent spectral changes in the substrate-saturated enzyme species resulted from a change in substrate binding (as claimed for CYP2B4[26]) could be ruled out for BM3. In accordance with the results from static measurements, the observed relaxation rates were shown to be independent of the NPG concentration. Thus, the different models for substrate-induced spin state transitions discussed for cytochrome P450 cam[25−27] could not be tested for BM3. In contrast to the observed rate constants, the relaxation amplitudes corresponded strictly to the concentration of NPG-bound enzyme and reproduced only 10% of the spectral change expected from static equilibrium experiments, suggesting that the observed slow process does not reflect the complete equilibrium process. This may be interpreted by combining the available structural

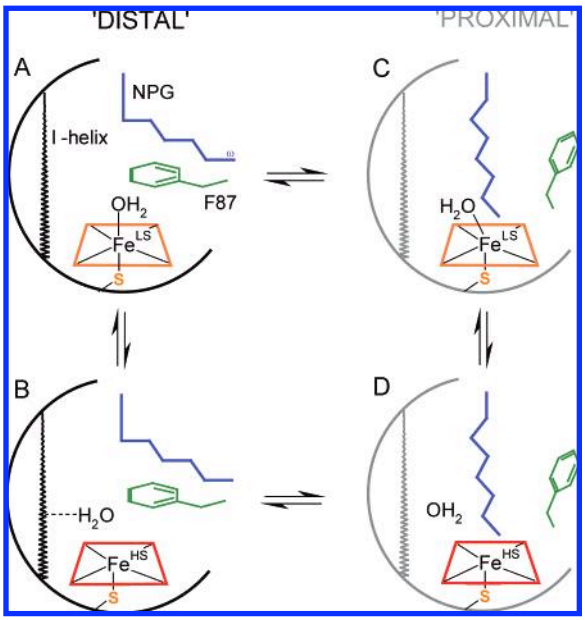

Figure 4. Schematic of the spin state equilibria in the proximal and distal NPG-binding modes. The distal binding mode (panels A and B) describes an ensemble of conformations with the NPG molecule (blue) bound at a position ~7.5 Å away from the heme iron and resembles the NPG-bound crystal structure.[45] For catalysis to occur, the ω end of the modified fatty acid has to approach the porphyrin ring yielding the proximal binding position[43,44,46] (panels C and D). Spin state equilibria (vertical) are likely to exist for both conformational ensembles and may be due to the partitioning of a water molecule between the heme iron yielding the LS state and the I-helix resulting in the HS state.[45] The repositioning of the substrate involves a conformational change of Phe87 (green), which separates the distally bound NPG molecule from the heme iron.[44] If this repositioning is slow, then a slow readjustment of the LS-HS equilibria (diagonal) will be observed in the T-jump. For more information see the text.

information from X-ray crystallography and solid-state NMR with published molecular dynamics simulations: The NPG-bound crystal structure[45] showed that the NPG molecule is bound at a position distal from the heme iron (shown schematically in Figure 4A,B) and it was proposed that the temperature-sensitive spin state equilibrium might be due to a partitioning of a water molecule between the heme iron (leading to LS enzyme, Figure 4A) and a binding site in the I-helix (yielding the HS state, Figure 4B). The resulting spin state transition is likely to occur at a rate similar to the substrate-free case, i.e., it may be a very fast process (≫10 000 s^{-1}). On the other hand, the NPG molecule has to move toward the iron for its hydroxylation during catalytic turnover.[43,44] Molecular dynamics calculations and NMR studies[44,47−49] indicated that the conformational change from the distal to the proximal binding position (A → C and B → D in Figure 4) does not only involve a repositioning of the fatty acid, but also a change in the rotameric conformation of Phe87. Thus, it is possible that a fast relaxation event resulting from the rapid partitioning of the water molecule may take place within the dead time of our data acquisition and may lead to a new equilibrium position shifted toward both the distal and the proximal HS species (Figure 4B,D). This equilibrium, which has already adapted to the new temperature, might then be disturbed once again by the slow repositioning of the fatty acid from the distal position (Figure 4A,B) to the proximal binding mode (Figure 4C,D). As a consequence, the resulting readjustment of the LS-HS equilibria (A → B and C → D in Figure 4) would yield a small spectral change observable in our T-jump experiments. The observed slow relaxation rate

would then reflect a complex combination of all slow as well as fast relaxation rates.

This conclusion was substantiated by analyzing the relaxation process in the BM3 mutant F87G. In agreement with the model suggested above, the observed relaxation process was ~3 times faster than that for the wild-type enzyme, indicating a significant contribution of Phe87 to a conformational change gating the actual spin state conversion. As the slow relaxation phase was not completely abolished, further amino acid residues in the active site may contribute to this rate-limiting process, or else the repositioning of the NPG molecule could be slow. The significant impact of Phe87 on the observed relaxation rate in BM3 underpins the proposed interpretation and is in accordance with the information from X-ray crystallography,[42,45] NMR studies,[43,46,48] as well as molecular dynamics simulations.[44,47,49] As a consequence, the equilibrium constants, which were determined for the NPG-bound enzyme species, cannot be employed to extract rate constants for the LS-to-HS transition and the reverse reaction, since these equilibrium constants reflect the entire schematic square. Nevertheless, the rate constants describing the distal-to-proximal transition are likely to occur on a similar time scale to those measured in the T-jump, i.e., between $\sim 10^2$ and 10^4 s^{-1}.

Conclusion

The presented study on spin state transitions in cytochrome P450 BM3 revealed a slow relaxation process, which was only observable in the NPG-bound enzyme, but not in the substrate-free species. Analysis of the F87G mutant demonstrated that this spin state conversion is partly rate-limited by a conformational change involving the side chain of Phe87. These findings suggest that the observed slow spin state conversion is conformationally gated by a transition from the distal binding site of the fatty acid to a position proximal to the heme iron.

Experimental Section

All chemicals were from Sigma-Aldrich (Poole, Dorset, UK). The substrate *N*-palmitoylglycine (NPG) was prepared as described in ref 45, with a purity >95%. Wild-type cytochrome P450 BM3 heme domain (wtBM3) and its mutant F87G (BM3-F87G) were expressed and purified essentially as described previously[50,51] with special care to purify only low-spin fractions; SDS-PAGE analysis showed that the degree of purity was >99%. The protein was stored in 50 mM Tris-HCl, 1 mM EDTA, 50% glycerol, pH 7.2 at −80 °C and transferred into the experimental buffer system (25 mM MOPS, 100 mM KCl, pH 7.0) by using a 10 mL disposable gel filtration column (BioRad, U.K.). Absolute BM3 concentrations were determined by formation of the reduced, carbon monoxide-bound enzyme species, using an optical difference extinction coefficient of $\Delta\epsilon_{450-490} = 91$ mM^{-1} cm^{-1} for the ferrous−CO complex relative to the ferrous enzyme.

All binding titrations and equilibrium experiments were performed in a Cary 50 UV−visible spectrophotometer (Varian Ltd, Oxford, U.K.), using a 1 cm path length cuvette thermally regulated with a peltier element (Varian Ltd, Oxford, U.K.) in combination with a pump-driven water cooling system. The data were fit to a quadratic binding equation (eq 1) yielding an observed (spectral) dissociation constant (K_d^{obs}):

$$\mathrm{AU} = \frac{1}{2}\epsilon_{EL}\{([E]_0 + [S]_0 + K_d^{obs}) - [([E]_0 + [S]_0 + K_d^{obs})^2 - 4[E]_0[S]_0]^{0.5}\} + \epsilon_E\left[[E]_0 - \frac{1}{2}\{([E]_0 + [S]_0 + K_d^{obs}) - [([E]_0 + [S]_0 + K_d^{obs})^2 - 4[E]_0[S]_0]^{0.5}\}\right] \quad (1)$$

where AU is the absorbance at the respective wavelength, ϵ_{EL} and ϵ_E are the extinction coefficients of the NPG-bound and substrate-free enzyme species, respectively, and $[E]_0$ and $[S]_0$ are the total enzyme and substrate concentration, respectively. The temperature dependence of the observed dissociation constants was analyzed by using the van't Hoff equation (eq 2):

$$\ln K_d^{obs} = \Delta H/RT - \Delta S/R; \qquad K_d^{obs} = \exp(\Delta G/RT) = [E^{LS}][S]/[E^{HS}S] \quad (2)$$

Spin state equilibrium constants were determined by measuring the Soret absorbance of the substrate-free and NPG-saturated enzymes between 10 and 40 °C, typically with 10 μM enzyme and NPG in a 2-fold excess when necessary. K_{eq} was determined by fitting the AU versus T data to:

$$\epsilon = \epsilon_{LS} + (\epsilon_{HS} - \epsilon_{LS})K_{eq}/(1 + K_{eq}) \quad (3)$$

with ϵ_{LS} and ϵ_{HS} the extinction coefficients for the pure low-spin and high-spin ferric enzyme, respectively. The reaction enthalpy, ΔH, and the entropy, ΔS, resulting from the fit, were then used to calculate the free energy, ΔG, and K_{eq}. For all curves, ϵ_{LS} was fixed to 94.5 mM^{-1} cm^{-1} (determined by fitting the substrate-free wild-type data to eq 3) and to 40 mM^{-1} cm^{-1} for pure high-spin enzyme (determined by fitting the NPG-bound wild-type data to eq 3) at 419 nm. This assumes that the presence of the substrate does not affect the extinction coefficient of pure high- and low-spin enzyme, but rather shifts the equilibrium between these states.

All T-jump experiments were carried out in a Hi-Tech Scientific TJ-64 capacitor T-jump instrument (TgK Scientific Ltd, Bradford on Avon, UK), using a tungsten lamp as light source, with a 100 μL quartz observation cell and an optical path length of 3 mm. A discharge voltage of 12 kV was used yielding a temperature jump of ~10 K.[53] The cell block was thermostated by using a circulating water bath and the starting temperature was set at 15 °C except for the acquisition of the Eyring data (see below). After each T-jump acquisition, the sample cell was allowed to cool to its thermostat temperature for at least 2 min. The maximum number of T-jumps performed with 100 μL protein solution was between 5 and 10. Experiments in the absence of substrate were performed with 30 μM P450 BM3, and 40 μM P450 was used for the experiments with NPG-bound protein. The action spectrum of substrate-free P450 BM3 was collected with use of a time constant of 10 ms; all other traces were acquired with a time constant of 0.1 ms. For each trace, more than 2000 data points were collected on a linear time scale. Typically, 15 to 20 traces were averaged; for the substrate-free trace acquired with a 0.1 ms time constant more than 40 traces were averaged. Traces were analyzed with the KinetAsyst software supplied by the instrument manufacturer (TgK Scientific Ltd, Bradford on Avon, UK) and were fitted to a single-exponential function. For a simple equilibrium between two substrate-bound or two substrate-free enzyme species it can be shown that the observed rate constant is the sum of the forward (k_f) and the reverse rate constant (k_r):[57,58]

$$E^{LS}S \underset{k_r}{\overset{k_f}{\rightleftharpoons}} E^{HS}S, \qquad k_{obs} = k_f + k_r \tag{4}$$

where $E^{LS}S$ and $E^{HS}S$ are NPG-bound enzyme species in the low-spin and the high-spin state, respectively. By using $K_{eq}^{sub} = [E^{HS}S]/[E^{LS}S] = k_f/k_r$, forward and reverse rate constants can be extracted from the observed rate constants given the equilibrium constant measured at the final temperature of the T-jump. The temperature dependence of the observed and calculated rate constants was analyzed with the Eyring equation. The errors in k_f and k_r were estimated by recalculating these rate constants from K_{eq}^{sub} redetermined assuming an error of ± 5 mM^{-1} cm^{-1} for ϵ_{LS} and ± 1 mM^{-1} cm^{-1} for ϵ_{HS}. The resulting rate constants were then reevaluated by using the Eyring equation and the difference between the recalculated activation parameters ($\Delta H^{\ddagger}$, $\Delta S^{\ddagger}$, and $\Delta G^{\ddagger}$) and the originally determined values yielded the error in these parameters.

Acknowledgment. We thank Ted King (TgK Scientific Ltd) for assistance with technical aspects of T-jump spectroscopy and for Ph.D. studentship funding (S.B.). We also thank the UK Biotechnology and Biological Sciences Research Council for project grant support. N.S.S. is a BBSRC Professorial Research Fellow. We thank Prof Paul M. Cullis (University of Leicester) for providing a sample of *N*-palmitoylglycine.

Supporting Information Available: Activation parameters calculated for the observed (k_{obs}) and microscopic rate constants (k_f, k_r) (Table S1), representative binding titration of *N*-palmitoylglycine to wtBM3 at 298 K (Figure S1), representative T-jump relaxation trace for substrate-free wtBM3 with use of a time constant of 10 ms (Figure S2), and Eyring plots of k_{obs}, k_f, and k_r for NPG-bound wtBM3 and BM3-F87G (Figure S3). This material is available free of charge via the Internet at http://pubs.acs.org.

References and Notes

(1) Ortiz de Montellano, P. R. *Cytochrome P450*: *Structure*, *Mechanism and Biochemistry*, 3rd ed.; Kluwer Academic/Plenum Press: New York, 2005; pp 377−530.

(2) Denisov, I. G.; Makris, T. M.; Sligar, S. G.; Schlichting, I. Structure and chemistry of cytochrome P450. *Chem. Rev.* **2005**, *105*, 2253−2277.

(3) Pylypenko, O.; Schlichting, I. Structural aspects of ligand binding to and electron transfer in bacterial and fungal P450s. *Annu. Rev. Biochem.* **2004**, *73*, 991−1018.

(4) Schenkman, J. B.; Remmer, H.; Estabrook, R. W. Spectral studies of drug interaction with hepatic microsomal cytochrome. *Mol. Pharmacol.* **1967**, *3*, 113−123.

(5) Schenkman, J. B. Effect of substrates on hepatic microsomal cytochrome P-450. *Hoppe-Seylers Z. Physiol. Chem.* **1968**, *349*, 1624−1628.

(6) Schenkman, J. B.; Sligar, S. G.; Cinti, D. L. Substrate interaction with cytochrome P-450. *Pharmacol. Ther.* **1981**, *12*, 43−71.

(7) Jefcoate, C. R.; Gaylor, J. L. Ligand interactions with hemoprotein P-450. II. Influence of phenobarbital and methylcholanthrene induction processes on P-450 spectra. *Biochemistry* **1969**, *8*, 3464−3472.

(8) Jefcoate, C. R.; Gaylor, J. L.; Calabrese, R. L. Ligand interactions with cytochrome P-450. I. Binding of primary amines. *Biochemistry* **1969**, *8*, 3455−3463.

(9) Griffin, B.; Peterson, J. A. Ethyl isocyanide complexes of bacterial cytochrome P-450. *Arch. Biochem. Biophys.* **1971**, *145*, 220−229.

(10) Raag, R.; Poulos, T. L. The structural basis for substrate-induced changes in redox potential and spin equilibrium in cytochrome P-450CAM. *Biochemistry* **1989**, *28*, 917−922.

(11) Daff, S. N.; Chapman, S. K.; Turner, K. L.; Holt, R. A.; Govindaraj, S.; Poulos, T. L.; Munro, A. W. Redox control of the catalytic cycle of flavocytochrome P-450 BM3. *Biochemistry* **1997**, *36*, 13816−13823.

(12) Dawson, J. H. Probing structure-function relations in heme-containing oxygenases and peroxidases. *Science* **1988**, *240*, 433−439.

(13) Fisher, M. T.; Sligar, S. Control of heme protein redox potential and reduction rate: Linear free energy relation between potential and ferric spin state equilibrium. *J. Am. Chem. Soc.* **1985**, *107*, 5018−5019.

(14) Sligar, S. Coupling of spin, substrate, and redox equilibria in cytochrome P450. *Biochemistry* **1976**, *15*, 5399−5406.

(15) Sligar, S. G.; Gunsalus, I. C. A thermodynamic model of regulation: modulation of redox equilibria in camphor monoxygenase. *Proc. Natl. Acad. Sci. U.S.A.* **1976**, *73*, 1078−1082.

(16) Wilson, G. S.; Tsibris, J. C.; Gunsalus, I. C. Electrochemical studies of putidaredoxin and its selenium analog. *J. Biol. Chem.* **1973**, *248*, 6059−6061.

(17) Schwarze, W.; Blanck, J.; Ristau, O.; Janig, G. R.; Pommerening, K.; Rein, H.; Ruckpaul, K. Spin state control of cytochrome P-450 reduction and catalytic activity in a reconstituted P-450 LM2 system as induced by a series of benzphetamine analogues. *Chem. Biol. Interact.* **1985**, *54*, 127−141.

(18) Rein, H.; Ristau, O.; Misselwitz, R.; Buder, E.; Ruckpaul, K. The importance of the spin equilibrium in cytochrome P-450 for the reduction rate of the heme iron. *Acta Biol. Med. Ger.* **1979**, *38*, 187−200.

(19) Backes, W. L.; Tamburini, P. P.; Jansson, I.; Gibson, G. G.; Sligar, S. G.; Schenkman, J. B. Kinetics of cytochrome P-450 reduction: evidence for faster reduction of the high-spin ferric state. *Biochemistry* **1985**, *24*, 5130−5136.

(20) Honeychurch, M. J.; Hill, A. O.; Wong, L. L. The thermodynamics and kinetics of electron transfer in the cytochrome P450cam enzyme system. *FEBS Lett.* **1999**, *451*, 351−353.

(21) Loida, P. J.; Sligar, S. G. Molecular recognition in cytochrome P-450: mechanism for the control of uncoupling reactions. *Biochemistry* **1993**, *32*, 11530−11538.

(22) Rein, H.; Ristau, O.; Friedrich, J.; Janig, G. R.; Ruckpaul, K. Evidence for the existence of a high spin-low spin equilibrium in liver microsomal cytochrome P-450. *FEBS Lett.* **1977**, *75*, 19−22.

(23) Cinti, D. L.; Sligar, S. G.; Gibson, G. G.; Schenkman, J. B. Temperature-dependent spin equilibrium of microsomal and solubilized cytochrome P-450 from rat liver. *Biochemistry* **1979**, *18*, 36−42.

(24) Cole, P. E.; Sligar, S. G. Temperature-jump measurement of the spin state relaxation rate of cytochrome P450cam. *FEBS Lett.* **1981**, *133*, 252−254.

(25) Fisher, M. T.; Sligar, S. G. Temperature jump relaxation kinetics of the P-450cam spin equilibrium. *Biochemistry* **1987**, *26*, 4797−4803.

(26) Narasimhulu, S. Substrate-induced spin-state transition in cytochrome P450LM2: a temperature-jump relaxation study. *Biochemistry* **1993**, *32*, 10344−10350.

(27) Narasimhulu, S.; Willcox, J. K. Temperature-jump relaxation kinetics of substrate-induced spin-state transition in cytochrome P450 (comparison of the wild-type and C334A mutant P450(CAM) and P450-(2B4)). *Arch. Biochem. Biophys.* **2001**, *388*, 198−206.

(28) Tsong, T. Y.; Yang, C. S. Rapid conformational changes of cytochrome P-450: effect of dimyristoyl lecithin. *Proc. Natl. Acad. Sci. U.S.A.* **1978**, *75*, 5955−5959.

(29) Narasimhulu, S. Differential behavior of the sub-sites of cytochrome 450 active site in binding of substrates, and products (implications for coupling/uncoupling). *Biochim. Biophys. Acta* **2007**, *1770*, 360−375.

(30) Ziegler, M.; Blanck, J.; Greschner, S.; Lenz, K.; Lau, A.; Ruckpaul, K. Kinetics of elementary steps in the cytochrome P-450 reaction sequence. V. Laser temperature-jump investigation of the spin relaxation kinetics of cytochrome P-450 LM2. *Biomed. Biochim. Acta* **1983**, *42*, 641−649.

(31) Narasimhulu, S. Significance of the steroid-induced type I spectral change in steroid C-21 hydroxylase system of bovine adrenocortical microsomes. *Arch. Biochem. Biophys.* **1971**, *147*, 391−404.

(32) Narasimhulu, S. Uncoupling of oxygen activation from hydroxylation in the steroid C-21 hydroxylase of bovine adrenocortical microsomes. *Arch. Biochem. Biophys.* **1971**, *147*, 384−390.

(33) Marden, M. C.; Hoa, G. H. P-450 binding to substrates camphor and linalool versus pressure. *Arch. Biochem. Biophys.* **1987**, *253*, 100−107.

(34) Narasimhulu, S. On the model controversy for substrate-induced spin-state transition in cytochrome P450: (a new perspective). *Endocr. Res.* **1993**, *19*, 223−258.

(35) Bell, S. G.; Chen, X.; Sowden, R. J.; Xu, F.; Williams, J. N.; Wong, L. L.; Rao, Z. Molecular recognition in (+)-α-pinene oxidation by cytochrome P450cam. *J. Am. Chem. Soc.* **2003**, *125*, 705−714.

(36) Poulos, T. L.; Finzel, B. C.; Howard, A. J. High-resolution crystal structure of cytochrome P450cam. *J. Mol. Biol.* **1987**, *195*, 687−700.

(37) Schlichting, I.; Jung, C.; Schulze, H. Crystal structure of cytochrome P-450cam complexed with the (1*S*)-camphor enantiomer. *FEBS Lett.* **1997**, *415*, 253−257.

(38) Wester, M. R.; Johnson, E. F.; Marques-Soares, C.; Dansette, P. M.; Mansuy, D.; Stout, C. D. Structure of a substrate complex of mammalian cytochrome P450 2C5 at 2.3 Å resolution: evidence for multiple substrate binding modes. *Biochemistry* **2003**, *42*, 6370−6379.

(39) Wester, M. R.; Johnson, E. F.; Marques-Soares, C.; Dijols, S.; Dansette, P. M.; Mansuy, D.; Stout, C. D. Structure of mammalian cytochrome P450 2C5 complexed with diclofenac at 2.1 Å resolution: evidence for an induced fit model of substrate binding. *Biochemistry* **2003**, *42*, 9335−9345.

(40) Wester, M. R.; Yano, J. K.; Schoch, G. A.; Yang, C.; Griffin, K. J.; Stout, C. D.; Johnson, E. F. The structure of human cytochrome P450 2C9 complexed with flurbiprofen at 2.0-Å resolution. *J. Biol. Chem.* **2004**, *279*, 35630−35637.

(41) Williams, P. A.; Cosme, J.; Vinkovic, D. M.; Ward, A.; Angove, H. C.; Day, P. J.; Vonrhein, C.; Tickle, I. J.; Jhoti, H. Crystal structures of human cytochrome P450 3A4 bound to metyrapone and progesterone. *Science* **2004**, *305*, 683−686.

(42) Li, H.; Poulos, T. L. The structure of the cytochrome P450BM-3 haem domain complexed with the fatty acid substrate, palmitoleic acid. *Nat. Struct. Biol.* **1997**, *4*, 140−146.

(43) Modi, S.; Primrose, W. U.; Boyle, J. M.; Gibson, C. F.; Lian, L. Y.; Roberts, G. C. NMR studies of substrate binding to cytochrome P450 BM3: comparisons to cytochrome P450 cam. *Biochemistry* **1995**, *34*, 8982−8988.

(44) Ravindranathan, K. P.; Gallicchio, E.; Friesner, R. A.; McDermott, A. E.; Levy, R. M. Conformational equilibrium of cytochrome P450 BM-3 complexed with *N*-palmitoylglycine: a replica exchange molecular dynamics study. *J. Am. Chem. Soc.* **2006**, *128*, 5786−5791.

(45) Haines, D. C.; Tomchick, D. R.; Machius, M.; Peterson, J. A. Pivotal role of water in the mechanism of P450BM-3. *Biochemistry* **2001**, *40*, 13456−13465.

(46) Modi, S.; Sutcliffe, M. J.; Primrose, W. U.; Lian, L. Y.; Roberts, G. C. The catalytic mechanism of cytochrome P450 BM3 involves a 6 Å movement of the bound substrate on reduction. *Nat. Struct. Biol.* **1996**, *3*, 414−417.

(47) Ravindranathan, K. P.; Gallicchio, E.; McDermott, A. E.; Levy, R. M. Conformational dynamics of substrate in the active site of cytochrome P450 BM-3/NPG complex: insights from NMR order parameters. *J. Am. Chem. Soc.* **2007**, *129*, 474−475.

(48) Jovanovic, T.; McDermott, A. E. Observation of ligand binding to cytochrome P450 BM-3 by means of solid-state NMR spectroscopy. *J. Am. Chem. Soc.* **2005**, *127*, 13816−13821.

(49) Jovanovic, T.; Farid, R.; Friesner, R. A.; McDermott, A. E. Thermal equilibrium of high- and low-spin forms of cytochrome P450 BM-3: repositioning of the substrate? *J. Am. Chem. Soc.* **2005**, *127*, 13548−13552.

(50) Miles, J. S.; Munro, A. W.; Rospendowski, B. N.; Smith, W. E.; McKnight, J.; Thomson, A. J. Domains of the catalytically self-sufficient cytochrome P-450 BM-3. Genetic construction, overexpression, purification and spectroscopic characterization. *Biochem. J.* **1992**, *288*, 503−509.

(51) Noble, M. A.; Miles, C. S.; Chapman, S. K.; Lysek, D. A.; MacKay, A. C.; Reid, G. A.; Hanzlik, R. P.; Munro, A. W. Roles of key active-site residues in flavocytochrome P450 BM3. *Biochem. J.* **1999**, *339*, 371−379.

(52) Quaroni, L. G.; Seward, H. E.; McLean, K. J.; Girvan, H. M.; Ost, T. W.; Noble, M. A.; Kelly, S. M.; Price, N. C.; Cheesman, M. R.; Smith, W. E.; Munro, A. W. Interaction of nitric oxide with cytochrome P450 BM3. *Biochemistry* **2004**, *43*, 16416−16431.

(53) Brenner, S.; Hay, S.; Scrutton, N. S. Application Note AN.019. T64. *Hi-Tech Scientific* **2006**.

(54) Sayed, Y.; Hornby, J. A.; Lopez, M.; Dirr, H. Thermodynamics of the ligandin function of human class Alpha, glutathione transferase A1-1: energetics of organic anion ligand binding. *Biochem. J.* **2002**, *363*, 341−346.

(55) Protasevich, I. I.; Brouillette, C. G.; Snow, M. E.; Dunham, S.; Rubin, J. R.; Gogliotti, R.; Siegel, K. Role of inhibitor aliphatic chain in the thermodynamics of inhibitor binding to Escherichia coli enoyl-ACP reductase and the Phe203Leu mutant: a proposed mechanism for drug resistance. *Biochemistry* **2004**, *43*, 13380−13389.

(56) Noy, N.; Xu, Z. J. Interactions of retinol with binding proteins: implications for the mechanism of uptake by cells. *Biochemistry* **1990**, *29*, 3878−3883.

(57) Bernasconi, C. F. *Relaxation kinetics*; Academic Press: New York, 1976.

(58) Fersht, A. *Structure and mechanism in protein science*: *A guide to enzyme catalysis and protein folding*; W. H. Freeman and Company: New York, 1999.